Volume 331, number 1,2, 134–140 FEBS 13024 September 1993

Astacins, serralysins, snake venom and matrix metalloproteinases exhibit identical zinc-binding environments (HEXXHXXGXXH and Met-turn) and topologies and should be grouped into a common family, the 'metzincins'

Wolfram Bode[a,*], Franz-Xaver Gomis-Rüth[b], Walter Stöckler[c]

[a]*Max-Planck-Institut für Biochemie, Abteilung für Strukturforschung, 82152 Martinsried (bei München), Germany*
[b]*Institut de Biologia Fonamental, Universitat Autònoma de Barcelona, 08193 Bellaterra, Barcelona, Spain*
[c]*Zoologisches Institut der Universität Heidelberg, Fachrichtung Physiologie, 69120 Heidelberg, Germany*

Received 9 August 1993

The X-ray crystal structures of two zinc endopeptidases, astacin from crayfish, and adamalysin II from snake venom, reveal a strong overall topological equivalence and virtually identical extended HEXXHXXGXXH zinc-binding segments, but in addition a methionine-containing turn of similar conformation (the 'Met-turn'), which forms a hydrophobic basis for the zinc ion and the three liganding histidine residues. These two features are also present in a similar arrangement in the matrix metalloproteinases (matrixins) and in the large bacterial *Serratia* proteinase-like peptidases (serralysins). We suggest that these four proteinases represent members of distinct subfamilies which can be grouped together in a family, for which we propose the designation, metzincins.

Astacin; Snake venom metalloproteinase; Matrix metalloproteinase; Thermolysin; Zinc endopeptidase family; Protein crystal structure

1. INTRODUCTION

The majority of zinc endopeptidases exhibit a characteristic HEXXH sequence integrated into an 'active-site helix'. The two histidine residues serve as zinc ligands, and the glutamic acid residue polarizes a water molecule involved in nucleophilic attack at the scissile peptide bond. These features were first examined in the structure of thermolysin [1,2]. In this proteinase and in some other closely related bacterial enzymes of the thermolysin family [3,4], another glutamic acid which is found 20 residues after the second histidine forms the fourth zinc ligand; this glutamic acid is likewise part of a conserved NEXXSD segment [5].

More recently, a considerable number of zinc endopeptidases have been sequenced where the zinc binding motif is extended to HEXXHXXGXXH [6–8]. These peptidases include the astacins [9–13], the snake venom zinc endopeptidases [14,15] now called the 'adamalysins' [16], the large bacterial *Serratia* protease-like extracellular metalloproteinases (serralysins; [17–19]), and the matrixins (matrix metalloproteinases, mammalian collagenases [20–22]).

We have solved the catalytic domain crystal structures of astacin and adamalysin II which can be considered prototypical representatives of two of these families [12,13,16]. These structures reveal that both proteinases exhibit (in spite of low overall sequence similarity) significant topological equivalence and especially a virtually identical zinc environment, including a common 'Met-turn'. A new structure analysis of the alkaline metalloproteinase isolated from *Pseudomonas aeruginosa* [23], belonging to the serralysins, shows that this proteinase shares these features. The matrixins also contain the extended zinc-binding signature and, in addition, conserved sequence motifs. Structure and sequence comparisons of these four metalloproteinase families (serralysins, astacins, adamalysins, and matrixins) give evidence that they can be grouped together into a common family which we suggest be called 'metzincins' due to the common zinc-binding region and methionine turn.

2. MATERIALS AND METHODS

The topological similarities of the crystal structures of astacin, adamalysin II and thermolysin have been investigated by visual inspection and using the program OVRLAP [24] which minimizes spatial distances as well as deviations of segmental orientations. Quite generous equivalence probability weights are chosen for the spatial and the orientational part ($E_1 = E_2 = 4.0$ Å).

Sequence alignments were performed using the program CLUSTAL implemented in the software package HUSAR at the Deutsches Krebsforschungszentrum (Heidelberg) as described in detail elsewhere [10]. These alignments were modified according to topological equivalences obtained by OVRLAP. The pre-aligned sequences were then

*Corresponding author. Fax: (49) (89) 8578 3516.

Published by Elsevier Science Publishers B V.

analyzed with the program PAUP version 3.0s for relationships and evolutionary divergence of the proteins involved [25].

3. RESULTS AND DISCUSSION

Astacin [12,13] and adamalysin II [16] are topologically similar molecules (Fig. 1a and b). Both consist of two domains separated by a long active-site cleft with the catalytic zinc ion at its basement. In both molecules, the 'upper' domain, essentially comprising the N-terminal chain parts is organized in relatively regular secondary structure elements, whereas the 'lower' domain formed by the C-terminal segment is organized in a more irregular manner, with both chains, however, ending in a C-terminal helix and an extended segment clamped to the upper domain. Furthermore, both upper domains consist essentially of a central highly twisted five-stranded β-pleated sheet of identical connectivities flanked by two long helices on its concave side. The adamalysin II sheet is, however, covered on its convex side by two additional helices and by longer multiple turn structures, thus giving rise to a shift of the zinc-binding residues to higher sequence numbers in adamalysin II (His-142, His-146, His-152) compared with astacin (His-92, His-96, His-102; see Table I).

Both polypeptide chains start in the lower domain. However, the N-terminus of astacin is completely buried in the lower domain, with its ammonium group involved in a solvent-mediated salt bridge formed with Glu-103 (the residue immediately following the third zinc-liganding histidine). As a consequence, the (active) astacin conformation seems to require a precisely processed N-terminus; N-terminally elongated molecules (proforms) presumably adopt quite different (and possibly inactive) conformations. This is clearly different from the situation in adamalysin II, where the N-terminus is freely exposed, allowing covalent coupling to other preceeding domains.

Both enzymes exibit virtually identical active-site environments (Fig. 1a; Fig. 1b; Fig. 2a). Adamalysin II and astacin have an 'active site helix' comprising the HEXXH zinc-binding consensus sequence, in common with thermolysin. In contrast to the bacterial enzyme, however, this helix terminates abruptly at a glycine residue (Gly-99 in astacin, Gly-149 in adamalysin II, see Table I) three residues after the second histidine residue, and the peptide chain turns sharply away from the helix axis towards the third zinc-liganding histidine of the 'signature' sequence (His-102 in astacin, His-152 in adamalysin II). The following residue of astacin, Glu-103, forms the aforementioned salt bridge with the N-terminus, thereby locking in the active site conformation; the corresponding Asp-153 of adamalysin II is in strong hydrogen bond contact with the active site basement (Met-turn, see below).

The peptide chains following these signature segments in both metalloproteinases comprise the much more irregularly folded lower domains. After a loop of 10 residues interconnected by a disulphide bridge, the adamalysin II chain turns back to the active site and forms a 1–4 tight turn comprising Cys-164–Ile-165–Met-166–Arg-167, with the methionine side chain providing a hydrophobic base beneath the three zinc-liganding histidine side chains (see Fig. 2b). On the other hand, the astacin chain, only after passing a multiple turn structure of 41 residues, enters a Ser-145–Ile-146–

Table I

Sequence alignment of three representatives of each subfamily of the metzincins

	Zinc-binding Signature	Met-turn
Astacin	TII**HE**LM**H**AI**G**FY**HE**HT (33)	EDYQYYSI**M**H**Y**GKYSF
Meprin α mouse	TIE**HE**IL**H**AL**G**FF**HE**QS (35)	TPYDYESL**M**H**Y**GPFSF
BMP1[a]	IVV**HE**LG**H**VV**G**FW**HE**HT (35)	ETYDFDSI**M**H**Y**ARNTF
Serralysin	TFT**HE**IG**H**AL**G**LS**HP**GD (16)	EDTRQFSL**M**S**Y**WSETN
Pseudomonas alk[b]	TLT**HE**IG**H**TL**G**LS**HP**GD (16)	EDTRAYSV**M**S**Y**WEEQN
Erwina b[c]	TLT**HE**IG**H**AL**G**LN**HP**GD (16)	EDTRQFSI**M**S**Y**WSEKN
Collagenase f	VAA**HE**LG**H**SL**G**LS**HS**TD	----IGAL**M**Y**P**SYTFS
Collagenase n	VAA**HE**FG**H**SL**G**LA**HS**SD	----PGAL**M**Y**P**NYAFR
Matrilysin	AAT**HE**LG**H**SL**G**MG**HS**SD	----PNAV**M**Y**P**TYGNG
Adamalysin II	TMA**HE**LG**H**NL**G**ME**HD**GK (2)	RGASL-CI**M**R**P**GLTPG
Atrolysin	TMA**HE**LG**H**NL**G**ME**HD**GK (2)	RGASL-CI**M**R**P**GLTKG
Trimerelysin	TMT**HE**LG**H**NL**G**ME**HD**DK (3)	CEA--CI**M**S**D**VISDK

Only the sections containing the zinc-binding histidine residues and the Met-loop are shown. The histidine zinc-ligands, the catalytically active glutamic acid residue, the residue directly following the third His ligand, the conserved Met residue, and the two positions after the Met are in bold face. The numbers in brackets indicate the intervening residues.

[a] Human bone morphogenetic protein I and a homologue from the nematide worm, *C aenorhabitis elegans*.

[b] *Pseudomonas aeruginosa* alkaline proteinase.

[c] *Erwinia chrysanthemi* protease b.

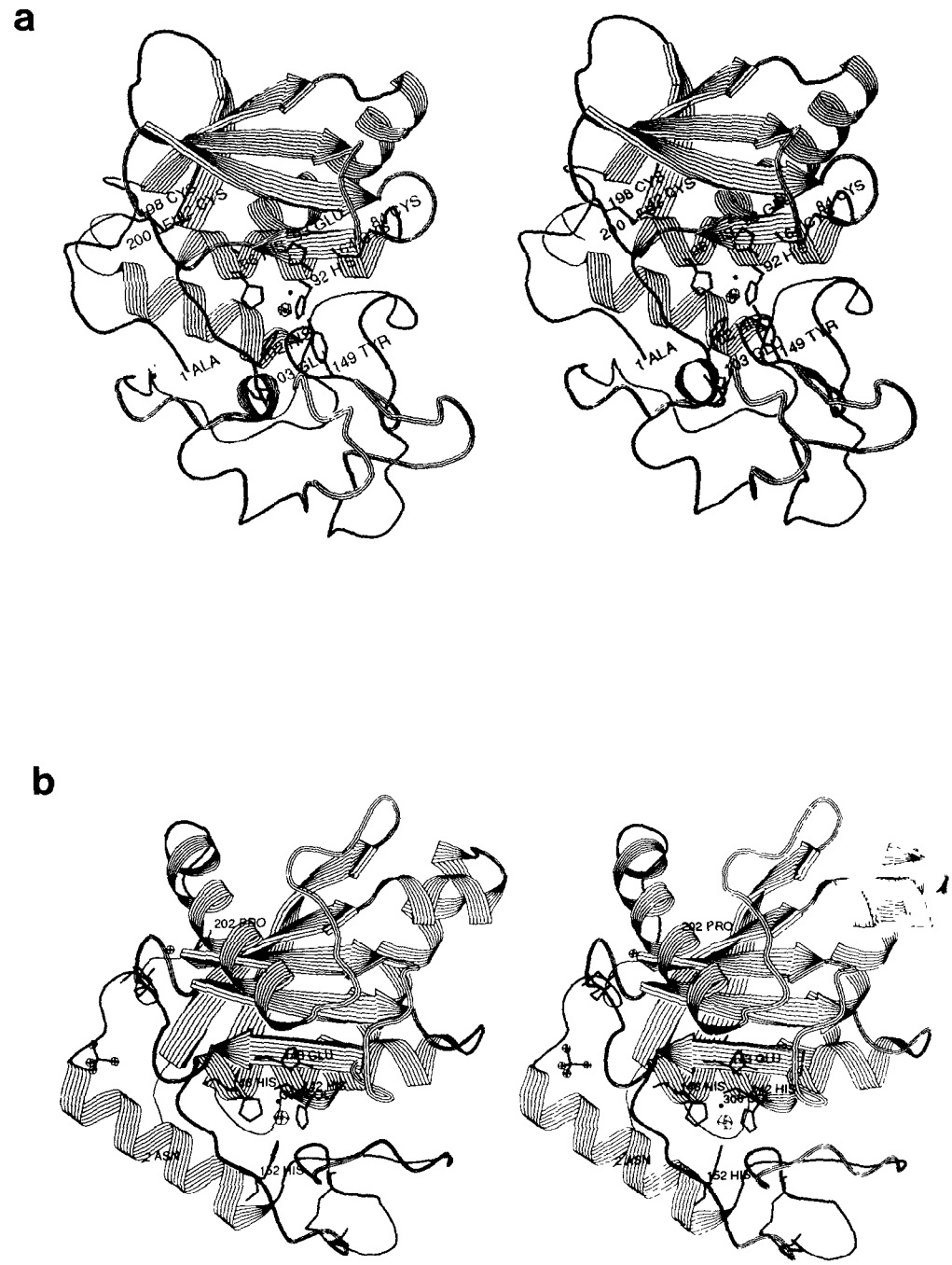

Fig. 1. Ribbon stereo plot of (a) astacin and (b) adamalysin II using RIBBON [30] (as modified by A. Karshikoff). Both molecules are shown in their 'standard orientation' [12], i.e. with the central active site cleft in the front running from left to right The zinc ion and a few residues which are particularly addressed in the text are shown in full and are extra labelled.

Met-147–His-148 tight turn of identical topology compared with the Met-turn of adamalysin II (Fig. 2a and Table I).

Subsequent to this Met-turn, the astacin and the adamalysin II chains deviate again. Whereas in the astacin chain Tyr-149 (the fifth zinc ligand) protrudes from the floor of the active site cleft towards the zinc ion, the corresponding Pro-168 of adamalysin II leaves the fifth zinc position freely accessible (Fig. 2a).

A structure comparison with the program OVRLAP and visual inspection reveal that about 106 of the 202 adamalysin II residues can be considered as topologically equivalent with astacin, with the relatively high rms deviations of 3.2 Å for their α carbon atoms. Of

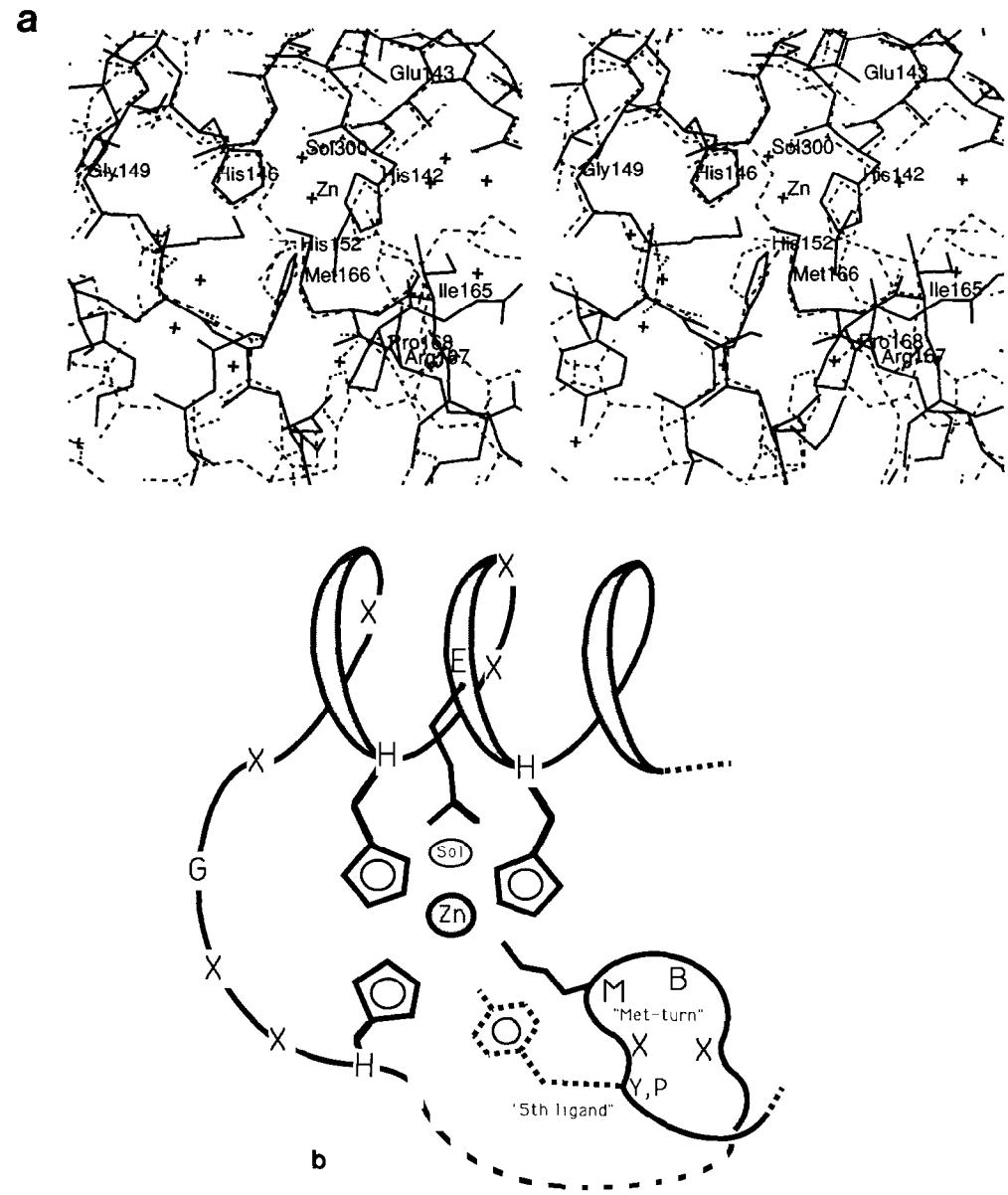

Fig. 2. (a) Stereoplot displaying the superimposed structures of adamalysin II (bold line) and astacin (dashed line) around their zinc-binding sites (using MAIN [31]). Only a few residues of adamalysin II are labelled. (b) Schematic representation of the zinc environment in the metzincins. Identical structures (zinc signature, Met-turn) are shown by a continuous line, variable features by a dashed chain trace. Standard orientation as in Fig. 1.

these equivalent residues, however, only 15 are identical, 7 of which are located in the extended zinc-binding consensus region and 3 in the Met-turn segment (Table I). The α-carbons of the 17 residues forming the 'zinc signature' and the Met-turn fit with rms deviations of only 0.35 Å.

The structure of the *Pseudomonas aeruginosa* alkaline proteinase [23], which is a representative of the serralysins, displays all structural elements characteristic for astacin and adamalysin II: (i) the five-stranded β-pleated sheet and the two adjacent large α-helices, (ii) the extended zinc-binding consensus sequence containing the three histidine residues and the intervening glycine residue, and (iii) the Met-turn comprising an SVMS sequence (see Table I). Due to the absence of coordinates, however, a quantitative comparison with astacin and adamalysin II is not yet possible. Here also, about half of the catalytic domain residues seem topologically equivalent, while only a few are identical.

The availability of three spatial structures of zinc-endopeptidases representing distinct subfamilies provide excellent tools for deciphering the structural relationships among these enzymes. We have in a first step aligned the corresponding amino acid sequences using the program CLUSTAL. We have then utilized the information obtained with OVRLAP by superimposing

the available three-dimensional structures for detection of topologically equivalent segments. These segments were arranged by hand and fixed. The intervening sequence regions were again aligned with CLUSTAL. Although there is no crystal structure available yet for the matrixin subfamily, we have also included this group of enzymes in our alignment, since they all contain the extended zinc-binding motif and share a conserved methionine residue seven positions downstream of the proposed third histidine zinc ligand. In the absence of such tertiary structure information, additional secondary structure predictions have been taken into account in order to achieve optimal alignment.

The alignment included 22 representatives belonging to the astacin-, adamalysin-, serralysin- and matrixin-subfamilies. A reduced section of the resulting alignment comprising the signature- and the Met-turn regions is displayed in Table I. All residues in a single row are considered to be topologically equivalent (either based on crystal structures or solely on sequence alignments and secondary structure predictions). Table II gives the lengths of the experimental or assumed topologically equivalent segments used for the alignment, the identical residues, and the percentage of identical residues within these topologically equivalent regions for four selected representatives as deduced from pairwise alignments. The overall sequence similarity is quite weak, compared with the sequence identities within the subfamilies that are generally above 30% and where very few single residue insertions and deletions are required for optimal assignment. In contrast, the percentage scores between the families lie in the region which Doolittle [26] has called the 'twilight zone' (between 15% and 25% sequence identity). However, by taking into account not only primary structure information, but also knowledge about zinc-binding environments (HEXXHXXGXXH and Met-turn), topologies from three-dimensional structures, and secondary structure predictions, these percentages (albeit low) are more meaningful. Surprisingly, there seems to be a much closer relationship between serralysins and matrixins than originally expected (26% identity within the topologically equivalent regions, compare Table II). Furthermore, astacin is also close to serralysin (22%), but most distant from human fibroblast collagenase (10%). The distance between adamalysin II and serralysin is likewise large (11%). The percentages of identical residues shared by adamalysin II with both astacin and collagenase are about 15%.

Table II

Percentage similarity scores between the different subfamilies of the metzincins calculated for four selected representatives

	AST	COL	SERR	ADA
AST	X	118 (12)	165 (37)	139 (20)
COL	10.2	X	166 (44)	133 (21)
SERR	22.4	26.5	X	158 (18)
ADA	14.3	15.8	11.3	X

AST stands for astacin, COL for human fibroblast collagenase, SERR for serralysin, and ADA for adamalysin II. The values in the upper triangle indicate the number of topologically and/or sequentially equivalent sequence positions and (in brackets) the identical residues within these equivalent stretches; those in the lower triangle indicate the percentage identity.

In all four subfamilies the zinc-binding segment follows the common sequence pattern HEBXHXBGBXHZ. The astacin and the adamalysin II structures offer an explanation for the conservation of these bulky, hydrophobic 'B' residues due to burying of their side chains in the hydrophobic cores of both molecules. The last residue in this extended signature, Z, which immediately follows the third histidine zinc ligand, differs in all 4 subfamilies, but seems to be strictly conserved within each subfamily (Glu in astacins, Asp in adamalysins, Ser in matrixins, and Pro in serralysins). Hence, as pointed out by Jiang and Bond [27], this residue may serve as a label to differentiate between the subfamilies (see Fig. 3). There are presumably functional reasons for the conservation of these Z residues within a given subfamily. In both the astacin and the adamalysin II structure this residue seems to be involved in active site stabilization; in astacin it is, in addition, presumably linked to activation.

As shown in Table I, the matrixins also exhibit a highly conserved Met-turn sequence, XBMX (almost exclusively confined to ALMY), five residues behind the third histidine. Simple model-building experiments show that if this connecting matrixin segment would run along the adamalysin II chain, the adjacent XBMX segment could be placed exactly as observed for astacins, adamalysins, and serralysins (Fig. 2b).

Thus, the unifying feature of the four subfamilies (besides the common zinc-binding signature) seems to be the Met-turn; this turn, together with the side chains of the residues at turn positions 2 (Ile, Leu or Val) and 3 (Met), obviously plays an important role in the structural integrity of the active site of these enzymes. The side chain of the following residue (at position 4 of the turn), in contrast, is, in all three known tertiary structures, directed away from the active site towards the bulk solvent. It varies not only between the 4 subfamilies, but also within 2 of the subfamilies (see Table I), which indicates its relative unimportance for the structural integrity.

The residue immediately following this 1,4-tight turn is found to be strictly conserved in 3 of these 4 subfamilies (tyrosine in all astacins and in all serralysins, but proline in all matrixins known so far), and less conserved (mostly proline) in the adamalysins (Table I). In the astacins, and very likely in the serralysins, this tyrosine represents the fifth zinc ligand (which in the structure of the present serralysin structure [23] seems to be slightly displaced by a bound peptide compared with its

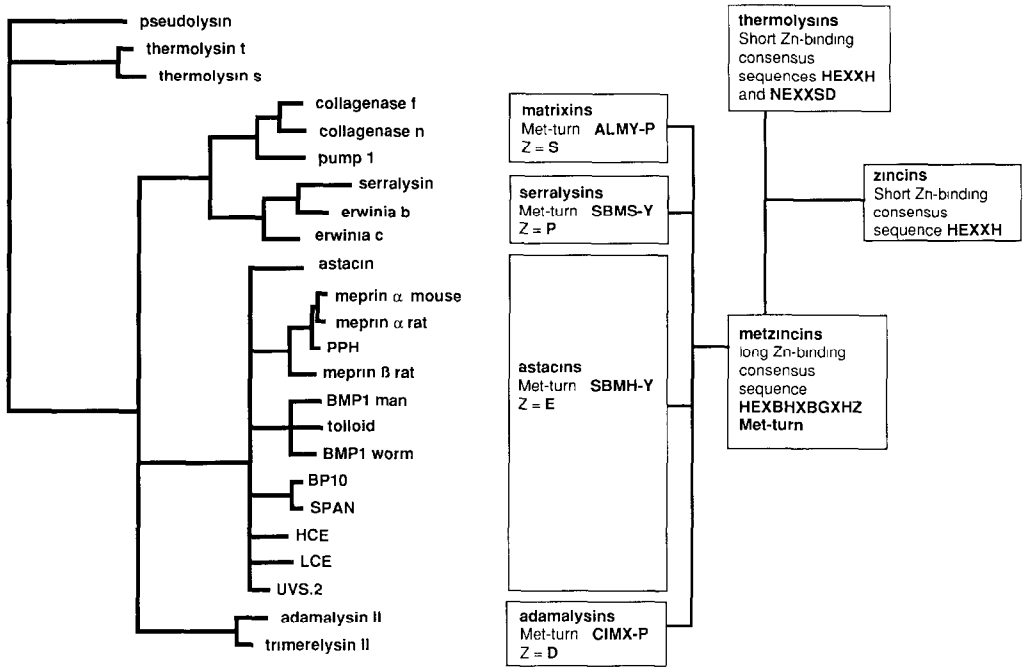

Fig. 3. Structural relationships between the zincins (HEXXH zinc-endopeptidases) and the metzincins (HEXBHXGBGXHZ/Met-turn metalloproteinases). Left panel: Phylogram of 24 zinc-endopeptidases as obtained by a maximum parsimony analysis of pre-aligned amino acid sequences using the program PAUP 3.0s [25]. The options employed were: branch and bound search, sequence addition: closest. The results of bootstrap analysis (100 replications) are depicted. The length of the horizontal lines reflect distance scores, i.e the number of amino acid substitutions. Right panel: Topological and sequential features typical for the zincins and metzincins. B stands for bulky, apolar residues; Z represents the residue following the third histidine zinc ligand. Pseudolysin, *Pseudomonas aeruginosa* elastase; thermolysin t, thermolysin from *Bacillus thermoproteolyticus*; thermolysin s, thermolysin from *Bacillus stearothermophilus*, collagenase f, human fibroblast collagenase; collagenase n, human neutrophil collagenase, pump1, matrilysin-'punctuated' or -putative metalloproteinase; serralysin, *Serratia* proteinase; erwinia b, *Erwinia chrysanthemi* protease b; erwinia c, *Erwinia chrysanthemi* protease c; PPH, human AbzOH-peptide hydrolase; BMP1, human bone morphogenetic protein 1 and a homologue from the nematode worm, *Caenorhabitis elegans*, BP10 and SPAN, blastula protein from sea urchin; HCE and LCE, fish embryonic hatching enzymes; UVS.2, frog embryonal protein; trimerelysin II, proteinase from *Trimeresurus flavoridis*. For references, see [10,12].

position in astacin). In adamalysin II, and very probably also in the matrixins, the equivalent main chain position is occupied by a proline, which does not extend into the zinc coordination sphere.

Thus, focussing on conserved tyrosine residues alone [27] may lead to incorrect alignments. Interestingly, the presence of a fifth tyrosine zinc ligand correlates with the absence of a 'cysteine switch region' [28,29] in the proparts of the corresponding metalloproteinases, presumably reflecting unwanted interference of this tyrosine residue with the mercapto-group of a cysteine peptide.

In comparing the metzincins with the archetypical zinc-endopeptidase thermolysin, it becomes apparent that there are some important similarities despite the overall structural variation. The helical part of the zinc binding signature of the metzincins is very similar to the corresponding XXHEXXHX segment in thermolysin. Furthermore, the upper domain of thermolysin contains a β-pleated sheet, the first four cleft-sided strands of which are topologically identical to their metzincin conterparts. However, the upper domain of thermolysin is much larger and has N-terminal appendices, and the active site helix extends far beyond the short HEXXH zinc-binding signature. Its polypeptide chain returns to the active site only after running through a much longer loop to donate the third zinc-liganding residue (Glu-166). The rest of the lower thermolysin domain is quite α-helical and bears no relation at all to any of the lower metzincin domains. Notably, in thermolysin the region approximately corresponding to the methionine sites of astacin and adamalysin II is occupied by the serine (Ser-169) of the consensus NEXXSD sequence which is otherwise structurally unrelated to the Met-turn.

A total of 78 adamalysin II and 62 astacin residues are topologically equivalent to thermolysin, with rms deviations of 3.5 Å and 2.8 Å, respectively, for the corresponding α-carbon atoms; 12 and 5, respectively, of these equivalent residues are chemically identical (the higher numbers of equivalent residues in the astacin–thermolysin superposition as compared to our previous paper [13] results from less rigorous equivalence parameters).

In summary this means that the metzincins are structurally related to the thermolysin-like enzymes forming an HEXXH zinc endopeptidase superfamily, for which

we suggest the name 'zincins'. This relatedness has been corroborated by including the thermolysin family into the structure based alignment mentioned above. This alignment has then been used to analyze the relationships between a total of 24 different zinc-endopeptidases using the maximum parsimony method [25]. As already anticipated, the enzymes form clusters corresponding to the different subfamilies. Also by this analysis the serralysins appear rather closely related to the matrixins, and the serralysin matrixin subcluster stands with equal rights with the astacin- and the adamalysin subclusters. These three subclusters are, however, more distantly related to the thermolysin-like proteinases (see Fig. 3).

The zincin superfamily comprises at the moment the thermolysins and the metzincins and is characterized by the short zinc-binding sequence, HEXXH. The metzincin family, in turn, is formed by the 4 subfamilies mentioned, i.e. the astacins, adamalysins, serralysins and matrixins, and has additionally in common the extension of the zinc-binding signature and the Met-turn. Prominent features, by which these subfamilies can be distinguished from one another, are the Z residue following the 'third' histidine zinc ligand, and the residue following the 1,4-tight Met-turn (see Fig. 3).

Acknowledgements: We thank Prof. Dr. Robert Huber, Prof. Dr. Robert Zwilling, and Prof. Dr. Francesc Xavier Avilés for their continuous encouragement, Dr. Lawrence Kress and Dr Ulrich Baumann for helpful comments. FXGR would like to acknowledge the help provided by a EMBO-long term fellowship. The financial support by the Sonderforschungsbereich 207 der Universitat München (WB) and the Deutsche Forschungsgemeinschaft (Sto 185/1-3) is gratefully acknowledged.

REFERENCES

[1] Matthews, B.W., Jansonius, J.N., Colman, P.M., Schoeborn, B.P. and Dupourge, D. (1972) Nature New Biol. 238, 37–41.
[2] Matthews, B W. (1988) Accts. Chem. Res. 21, 333–340
[3] Thayer, M.M., Flaherty, K.M. and McKay, D.B. (1991) J. Mol. Biol. 266, 2864–2871.
[4] Pauptit, R.A., Karlsson, R., Picot, D., Jenkins, J.A., Niklaus-Reimer, A.S. and Jansonius, J.N. (1988) J. Mol. Biol. 199, 525–537.
[5] Titani, K., Hermodson, M.A., Ericsson, L.H., Walsh, K.A. and Neurath, H. (1972) Nature New Biol. 238, 35–37.
[6] Stöcker, W., Ng, M. and Auld, D.S. (1990) Biochemistry 29, 10418–10425.
[7] Murphy, G.J.P., Murphy, G. and Reynolds, J.J. (1991) FEBS Lett. 289, 4–7.
[8] Rawlings, N.D and Barrett, A.J. (1993) Biochem. J. 290, 205–218.
[9] Stöcker, W., Sauer, B. and Zwilling, R. (1991) Biol. Chem. Hoppe-Seyler 372, 385–392.
[10] Stöcker, W., Gomis-Rüth, F.X., Bode, W. and Zwilling, R (1993) Eur J Biochem. 214, 215–231.
[11] Dumermuth, E., Sterchi, E.E , Jiang, W., Wolz, R.L., Bond, J.S., Flannery, A. and Beynon, R J (1990) J. Biol. Chem. 266, 21381–21385.
[12] Bode, W., Gomis-Rüth, F.X , Huber, R , Zwilling, R. and Stöcker, W. (1992) Nature 358, 164–167.
[13] Gomis-Rüth, F X., Stöcker, W., Huber, R., Zwilling, R. and Bode, W. (1993) J. Mol. Biol. 229, 945–968.
[14] Shannon, J.D., Baramova, E N , Bjarnason, J.B. and Fox, J.W. (1989) J. Biol. Chem. 264, 11575–11583.
[15] Kini, R.M. and Evans, H.J. (1992) Toxicon 30, 265–293.
[16] Gomis-Rüth, F.X., Kress, L.F. and Bode, W. (1993) EMBO J. (in press).
[17] Nakahama, K., Yoshimura, K., Marumoto, R., Kikuchi, M., Lee, I.S., Hase, T and Matsubara, H. (1986) Nucleic Acids Res. 14, 5843–5855.
[18] Delepelaire, P and Wandersman, C. (1989) J. Biol. Chem. 264, 9083–9089.
[19] Duong, F., Lazdunski, A., Cami, B. and Murgier, M. (1992) Gene 121, 47–54.
[20] Matrisian, L.M. (1990) Trends Genet. 6, 121–125.
[21] Woessner, Jr. J.F. (1991) FASEB J. 5, 2145–2154
[22] Nagase, H., Barrett, A.J and Woessner, Jr. J F. (1992) Matrix (Suppl. No. 1), 421–424.
[23] Baumann, U., Wu, S , Flaherty, K M and McKay, D.B. (1993) EMBO J. (in press)
[24] Rossmann, M.G. and Argos, P. (1975) J. Biol Chem. 250, 7525–7532.
[25] Swafford, D.L. (1991) PAP: Phylogenetic analysis using parsimony; version 3.0s. Champaign, Illinois Natural History Survey
[26] Doolittle, R.F. (1985) Sci. Am 253, 74–83
[27] Jiang, W. and Bond, J.S. (1992) FEBS Lett 312, 110–114.
[28] Springman, E.B., Angleton, E.L., Birkedal-Hansen, H. and Van Wart, H.E. (1990) Proc. Natl. Acad. Sci. USA 87, 364–368.
[29] Hite, L.A., Fox, J.W and Bjarnason, J.B. (1992) Biol. Chem. Hoppe-Seyler 373, 381–385
[30] Priestle, J.P (1988) J. Appl. Chrystallogr. 21, 572–576.
[31] Turk, D. (1992) Ph.D. Thesis, University of Munich, Munich.

NOTE ADDED IN PROOF

Our newly determined catalytic domain structure of a human collagenase now confirms that the collagenases share the characteristic overall topology and identical zinc environment with the other metzincins, and exhibit an active-site geometry very similar to the adamalysins.